CONF-9106262--2

DE91 017153

CALCULATIONS OF PAIR PRODUCTION BY MONTE CARLO METHODS

C. Bottcher and M. R. Strayer
Oak Ridge National Laboratory
Oak Ridge, TN 37831-6373

DISCLAIMER

to be published in

Proceedings of

Third IMACS Symposium on Computational Acoustics
Cambridge, Massachusetts
June 26-28, 1991

MASTER

CALCULATIONS OF PAIR PRODUCTION BY MONTE CARLO METHODS

C. Bottcher and M. R. Strayer

Center for Computationally Intensive Physics

Physics Division, Oak Ridge National Laboratory

Oak Ridge, TN 37831

ABSTRACT

We describe some of the technical design issues associated with the production of particle-antiparticle pairs in very large accelerators. To answer these questions requires extensive calculation of Feynman diagrams, in effect multi-dimensional integrals, which we evaluate by Monte Carlo methods on a variety of supercomputers. We present some portable algorithms for generating random numbers on vector and parallel architecture machines.

1. INTRODUCTION

One of the most visible, if esoteric, fields of science at the present day is the attempt to probe the structure of matter at very short distances by accelerating particles to great energies. The energies must be considerable in order to overcome the repulsive forces which operate at small distances. Another way of translating the distance scale is to estimate the time when the early universe developed fluctuations of that size. The projected *Superconducting Supercollider* (SSC) to be built in Texas will reach energies of 20 TeV, corresponding to distances of 10^{-21}cm or a time when the universe was a millisecond old [1]. The SSC is designed to accelerate protons, but two other types of accelerator are proposed. The Relativistic Heavy Ion Collider (RHIC) at Brookhaven National Laboratory is similar in concept to the SSC, but it will accelerate heavier nuclei, up to uranium, at lower energies of 100 GeV per nucleon [2]. Yet other proposals are concerned with accelerating bunches of electrons in linear colliders, at energies of up to a TeV; if built, this would be the *Tevatron Linear Collider* (TLC). Our current interest is chiefly in problems connected with the RHIC machine, though similar considerations apply to the others [3]. We find that large-scale numerical calculations are required, of a type well suited to supercomputers, including those with parallel architectures.

The plan of this paper is to outline the physics of relativistic heavy-ion collisions and colliders in Section 2, to describe the Feynman-Monte Carlo technique with some examples in Section 3, and finally in Section 4 to discuss the generation of random numbers on vector and parallel architecture computers.

2. RELATIVISTIC HEAVY-ION COLLISIONS

A highly schematic view of a collider, such as RHIC, is presented in Fig. 1. The essential components are two rings, one above the other, capable of accelerating and storing particles by combinations of electromagnetic fields. They may be several miles in diameter. The rings are successively injected with counter-rotating beams of ions which can intersect in crossing regions, of which four are included in the figure [2].

During the collision of heavy ions at relativistic velocities, large transient electromagnetic fields are formed in a space-time region near the collision. According to the theories of Dirac, Feynman and Schwinger, amply confirmed by experiments, these fields are sufficiently intense to produce large numbers of particle-antiparticle pairs from the vacuum. The particles might be electron, muon, or tauon pairs, or other more exotic particles, including, in principle, the unconfirmed Higgs boson [4]. In a collider geometry each ion has a Lorentz contraction γ given by

$$\gamma = \frac{1}{\sqrt{1-\beta^2}} \simeq (E/A)\ \mathrm{GeV}. \tag{1}$$

The equivalent fixed target energy is $\gamma_{\mathrm{FT}} = 2\gamma^2 - 1$, or 2×10^4 for RHIC. It is this large number which determines the tranverse field in the frame of one nucleus, and hence the rate of pair production. Figure 1 illustrates schematically the production of a pair from the electromagetic fields of colliding ions,

$$\mathcal{E}, \mathcal{B} \sim \frac{Z\gamma_{\mathrm{FT}}}{b^2}. \tag{2}$$

The electric field peaks at the distance of closest approach b where it is pre-

dominantly transverse. The figure also indicates the possibility that the negative member of the pair may be captured onto one of the nuclei. If the fields act coherently, the rate of pair production scales as Z^4/m^2, where Z is the nuclear charge and m the mass of the emitted particles. This predicts that the cross sections for electron-positron production are larger than any other electromagnetic or nuclear process.

The design of accelerators is a mature area of great fascination, combining electromagnetism and classical mechanics [3]. Only recently have design issues arisen which require quantum mechanical calculations of processes on a microscopic scale. We shall discuss two such processes.

- Free electron pairs produced by electromagnetic fields create large backgrounds in detectors searching for other phenomena. Detailed calculations are needed for design studies to minimize the backgrounds.

- If the electron in an electron-positron pair is captured by one of the ions, that ion will be lost from the beam. This is *the leading beam destruction mechanism* in heavy-ion colliders, and a reliable estimate is needed to ensure that the beams will live for several hours without expensive refilling.

Both phenomena come to be important in a curious way. Heavy-ion colliders are constructed to explore nuclear matter at great temperatures and pressures. Yet because heavy ions are highly charged, the inevitable competing electromagnetic processes may be larger than the nuclear, especially if the coherence factor Z^4 is

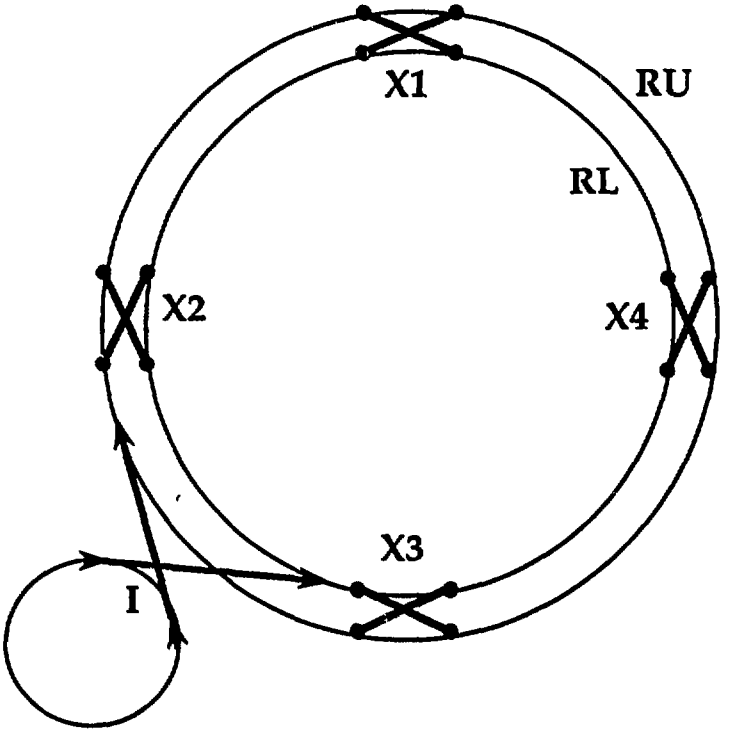

Fig. 1. A Relativistic Heavy-Ion Collider: the upper and lower rings (RU and RL) are injected from another ring I. The beams intersect in crossing regions X1–X4.

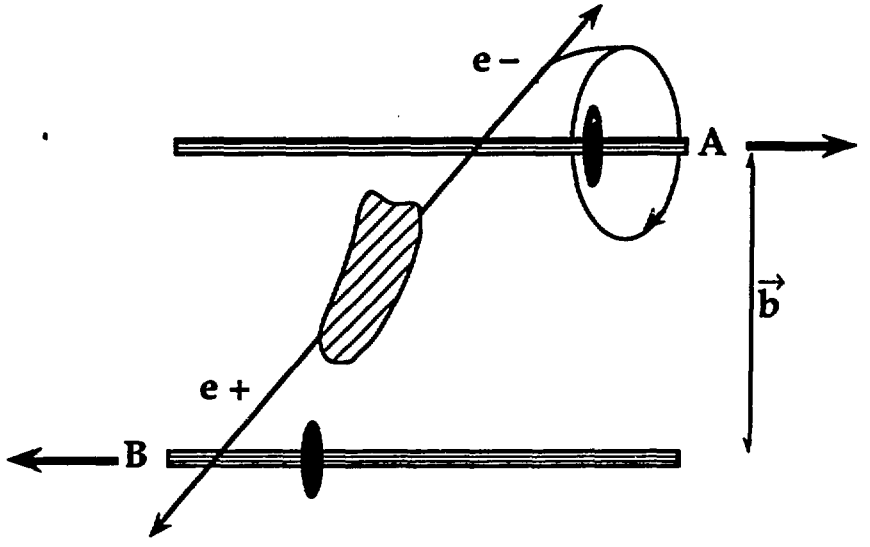

Fig. 2. Pair production in a relativistic heavy-ion collision, including the possibility of capture: the region of intense electromagnetic fields is indicated by cross-hatching.

operative. This suggests that if the electromagnetic processes are so large, they might be turned to advantage as a way of looking for fundamental phenomena, such as the production of the Higgs boson. We shall examine this possibility as a third example of our techniques, to be described in the following section.

To provide a frame of reference, Table 1 lists γ and γ_{FT} in round numbers for present and forseeable heavy-ion colliders. Some fixed-target machines (AGS and SPS) are listed as though they were colliders. No plans exist at the time of writing to inject heavy ions into the largest machines, the SSC and ELOISATRON.

Table 1

Energies of Heavy-Ion Colliders.

Facility	Location	γ	γ_{FT}
AGS	Brookhaven	3	17
SPS	CERN, Geneva	10	200
RHIC	Brookhaven	100	2×10^4
LHC	CERN, Geneva	2000	8×10^6
SSC	Texas	8000	1.3×10^7
ELOISATRON	European, proposed	4×10^4	3×10^9

Some explanation of terminology and units may be helpful. The cross section for any process is defined as the number of occurrences per second divided by the flux in the incident beam per second per unit area. The usual unit in nuclear physics is the "barn" (b) = 10^{-24} cm^2; the "nanobarn" (nb) = 10^{-33} cm^2. In colliders, these numbers are converted back into occurrences (or "events") when multiplied

by the "luminosity" of a particular accelerator measured in cm^{-2} sec^{-1}. Typical collider luminosities lie between 10^{26} and $10^{36} cm^{-2}$ sec^{-1}.

3. THE FEYNMAN MONTE CARLO METHOD

3.1 Formalism

We shall now sketch the theoretical background of pair production calculations. Textbooks may be consulted for more details [5]. We use standard covariant notation, $x^\mu = (ct, \vec{r})$ and the metric $x^2 = x \cdot x = (ct)^2 - \vec{r}^2$. It should be understood that the electromagnetic fields are treated classically. They are derived from the heavy-ion current $J^\mu(x)$ through Maxwell's equations for the four-potential $A^\mu(x)$,

$$\Box A^\mu = J^\mu \,. \tag{3}$$

The Lagrangian describing their interaction with the quantal fields of particles and antiparticles $\psi, \bar{\psi}$ is written,

$$\mathcal{L}_{\rm int}(x) = e : \bar{\psi}(x)\gamma^\mu\psi(x) : A_\mu(x) \,, \tag{4}$$

whence the S-matrix is given by the formal expression

$$\mathcal{S} = \mathrm{Texp}[i \int d^4x \, \mathcal{L}_{\rm int}] \,. \tag{5}$$

The ordered exponential in (5) is an instruction to expand what follows in a series of terms described by Feynman diagrams. We are mostly concerned with the leading (second order) term in pair production, leading to the cross section for producing a pair with four-momenta (k_1, k_2)

$$\sigma = \int d^2b \left| \langle k_1 k_2 | S^{(2)} | O \rangle \right|^2 . \tag{6}$$

In this formula the impact parameter $\vec{b}$ is the transverse distance between the trajectories shown in Fig. 2, and $|O\rangle$ denotes the vacuum state.

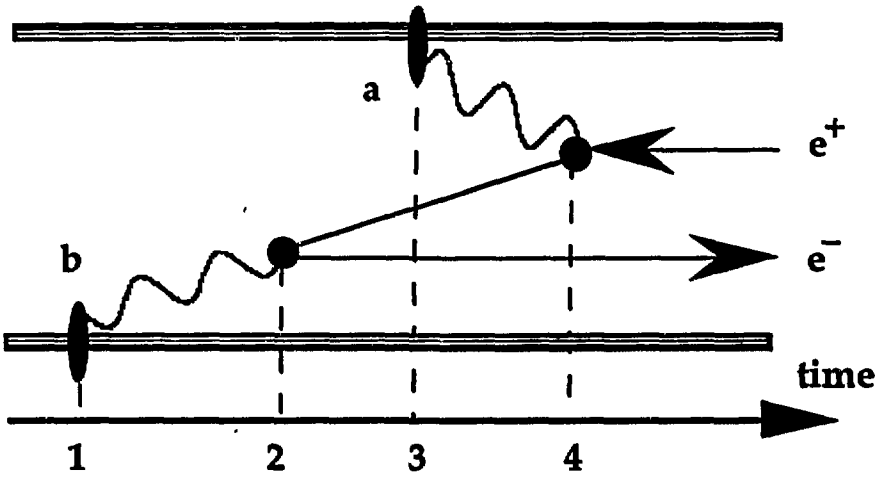

Fig. 3. Feynman diagram for pair production in "exploded" form.

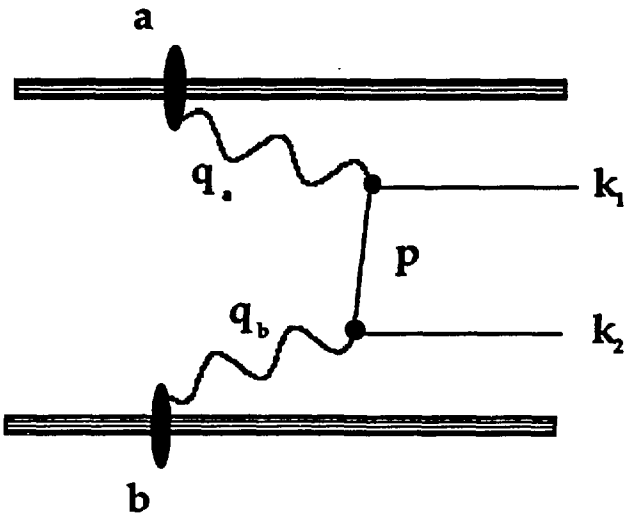

Fig. 4. Feynman diagram for pair production in standard form.

The term $\mathcal{S}^{(2)}$ occurring in (6) is described by the Feynman diagram, shown in "exploded" form in Fig. 3. The diagram is a time history of the production of a pair: at times **1** and **3** the nuclei emit photons, and at times **2** and **4** the photons create pairs. The more conventional view is given in Fig. 4.

To evaluate $\mathcal{S}^{(2)}$, each vertex and line in the diagram in Fig. 4 is associated with a factor according to prescribed rules. In particular, the vertex associated with the classical field of nucleus 'a' gives a factor which is, within some normalization, the Fourier transform of the four-vector,

$$A_{\rm a}^{\mu}(q) = Z_{\rm a}U_{\rm a}^{\mu}\left[\frac{F_{\rm a}(-q^2)}{-q^2}\right] 2\pi\delta(q^0-\beta q^z)\exp(-i\vec{q}_\perp\cdot\vec{b}/2)\,. \tag{7}$$

The photon four-momentum is denoted by q; the charge, speed and four-velocity of the ion are $Z_{\rm a}$, β and $U_{\rm a}^{\mu}$ respectively. A crucial role is played by the form factor $F(-q^2)$, which is essentially the Fourier transform of the nuclear density, normalized so that $F(0)=1$. At momenta greater than $R_{\rm nuc}^{-1}$, where $R_{\rm nuc}$ is the nuclear radius, the form factor falls off rapidly. Most of our applications lie in this régime.

The cross section (6) is then given by an eight-dimensional integral,

$$\sigma = \left[\frac{Z_{\rm a}Z_{\rm b}}{2\beta}\right]^2 \int \frac{d^3k_1 d^3k_2}{(2\pi)^6 2E_1 2E_2}\frac{d^2q_\perp}{(2\pi)^2}\left[\frac{F_{\rm a}(-q_{\rm a}^2)}{-q_{\rm a}^2}\frac{F_{\rm b}(-q_{\rm b}^2)}{-q_{\rm b}^2}\right]^2$$
$$\times\left|\bar{u}(k_1)\left[\not{A}_{\rm a}\frac{1}{\not{p}-m}\not{A}_{\rm b}+\not{A}_{\rm b}\frac{1}{\not{p}'-m}\not{A}_{\rm a}\right]v(k_2)\right|^2\,. \tag{8}$$

In this expression the slashed quantities are 4×4 matrices constructed from the components of four-vectors, while u and v are four-component spinors. The photon momenta $q_{\rm a}, q_{\rm b}, q_{\rm a\perp} = q_{\rm b\perp}$ and the intermediate lepton momenta p, p' can all be

expressed in terms of k_1, k_2. From the perspective of numerical calculation, the salient feature of (8) is that it may be cast as a finite sum (though of several hundred terms)

$$\sigma = \sum_K \mathcal{A}_K \, \mathcal{B}_K(k_1, k_2) \,, \tag{9}$$

where the $\mathcal{A}_K$ are constants from the spinor algebra, and the $\mathcal{B}_K$ are simple algebraic functions of the integration variables. This is a form well suited to evaluation on vector machines.

3.2 Applications

The integrand in (8) is positive everywhere so that the integral is suited to evaluation by Monte Carlo methods [6]. By appropriately mapping the variables, we can write (8) in the form

$$\sigma = \int_0^1 dy_1 \cdots \int_0^1 dy_8 \, f(y_1, \ldots, y_8) \,. \tag{10}$$

where f is a reasonably smooth function. The Monte Carlo estimate of σ derived from a sample of N uniformly distributed random points is thus

$$\bar{\sigma} = \frac{1}{N} \sum_{j=1}^{N} f(y_1^{(j)}, \ldots, y_8^{(j)}) \,, \tag{11}$$

with an estimated error Δ given by

$$\Delta^2 = \frac{1}{N^2 \bar{\sigma}^2} \sum_{j=1}^{N} |f(y_1^{(j)}, \ldots, y_8^{(j)}) - \bar{\sigma}|^2 \,. \tag{12}$$

For a typical problem (the calculation of Fig. 6, below), Fig. 5 shows the decrease in error with the number of points, which closely follows an $N^{-1/2}$ law. The points

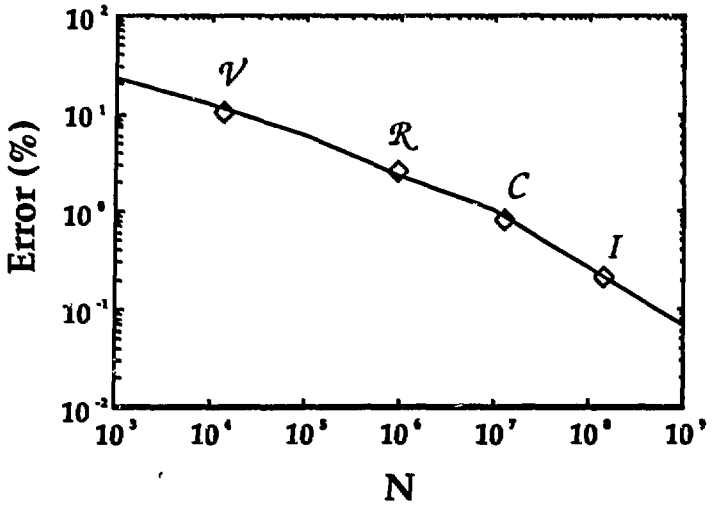

Fig. 5. Variation of residual Monte Carlo error with the number of points. The letters indicate the point reached after three minutes on several machines: V, Vax 785: R, IBM Risc 6000; C, Cray 2; I, Intel 860 hypercube.

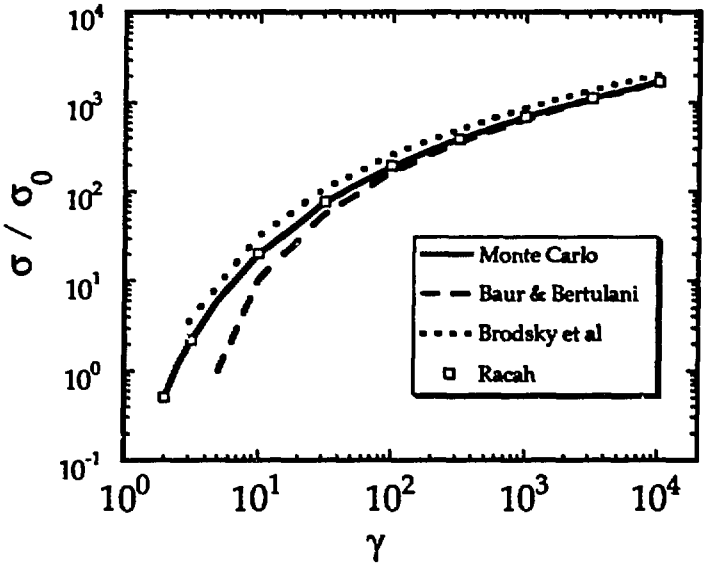

Fig. 6. Total cross section for electron-positron production in a variety of approximations. The scale cross section is σ_0 = 165b, a natural unit for many electromagnetic processes. .

reached after three minutes of computation on a range of computers are indicated on the curve.

As a test of the method, we show in Fig. 6 the variation of the two-photon cross section for electron-positron production by unit point charges calculated in various approximations [6,7]. The Monte Carlo and Racah results are practically identical and may be regarded as exact. This result scales rigorously with mass and charge as Z^4/m^2 for point charges and provides an upper bound for any calculation including a form factor. Subsequent examples involve complicated form factors and constraints on the region of integration which rule out analytic treatments.

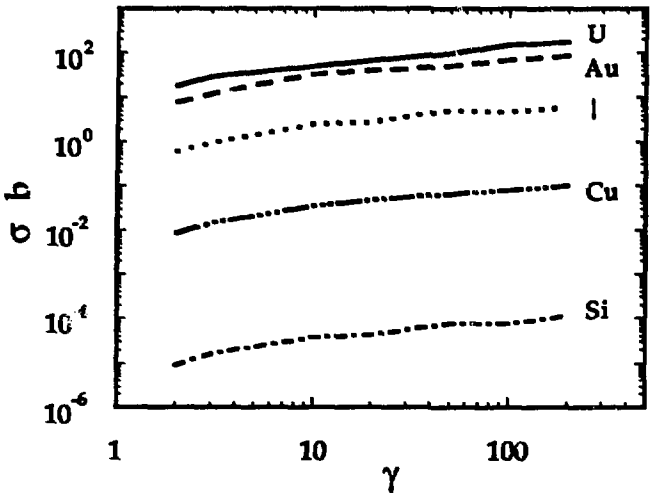

Fig. 7. Capture cross sections for collisions between symmetric ion pairs as a function of energy.

We now turn to consider some applied problems [8]. The capture cross section may be calculated using an extension of (8). The results are shown in Fig. 7 for collisions of a range of symmetric ion pairs. The number calculated for gold in

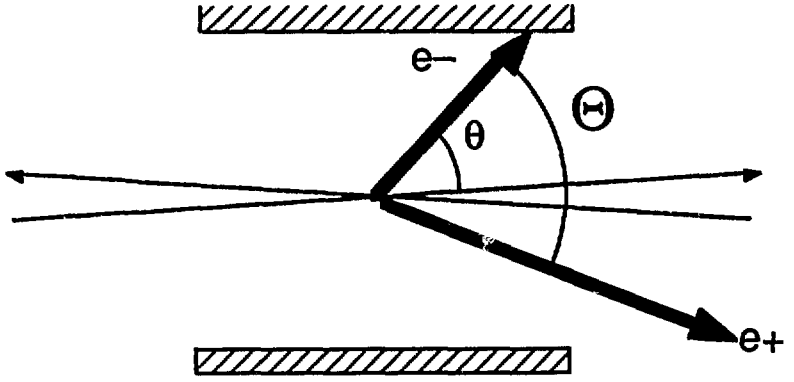

Fig. 8. Geometry of detectors in a collider experiment, distinguishing between the acceptance angle θ for a single particle, and the angle Θ subtended by the two members of a pair.

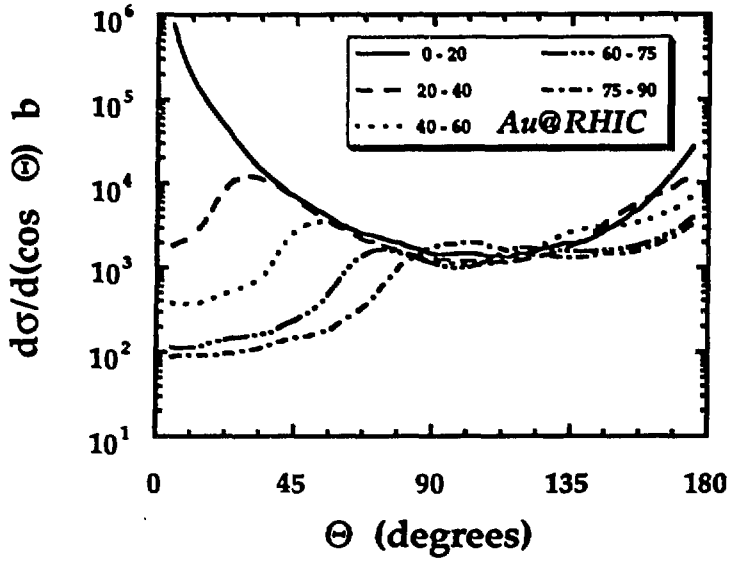

Fig. 9. Differential cross sections as a function of the pair angle Θ for a variety of cuts on the acceptance angle of singles θ.

RHIC (100 GeV/nucleon) implies a beam lifetime of 10 hours which is highly satisfactory [9]. As we mentioned above, electron-positron pairs may be an unwelcome background for many nuclear experiments, so that detector designers seek out peculiarities, or "signatures" which can be used to distinguish genuine from spurious

signals. One such signature is the angle Θ between two members of a pair when it is known that one member has been produced at an angle θ. A typical detector geometry is illustrated in Fig. 8: the detector is a cylinder around the crossing region of the beams, so that a single particle is only detected if θ is greater than about 40 degrees. Figure 8 shows the distribution of Θ for different selections, or "cuts," on θ, again for Au in RHIC (100 GeV/nucleon) [10].

As a final example, we take a very fundamental process, the electromagnetic production of the Higgs boson — the crucial, yet unobserved, building block of the standard model of particle physics [11,12]. The question to answer is whether the electromagnetic process for heavy ions is competitive with nuclear processes for proton collisions, in virtue of the coherence factor of Z^4 to which we have referred several times. The process in question is described by the Feynman "triangle" diagram Fig. 10, in which two pairs merge to produce the scalar Higgs. Since

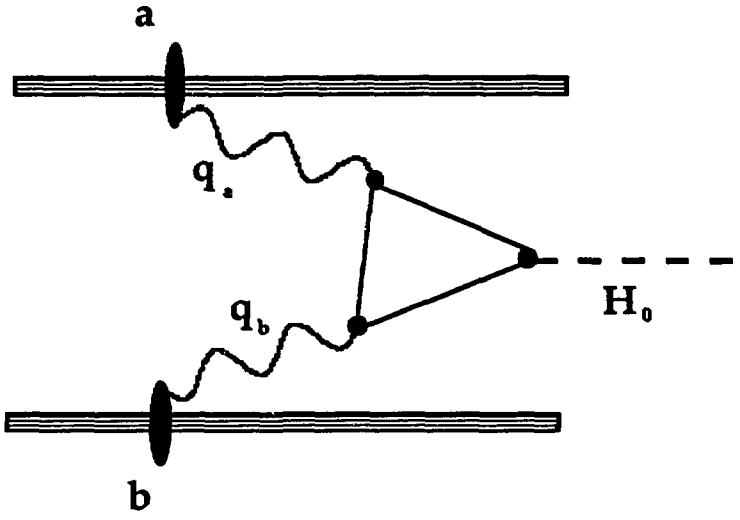

Fig. 10. Feynman diagram for Higgs production.

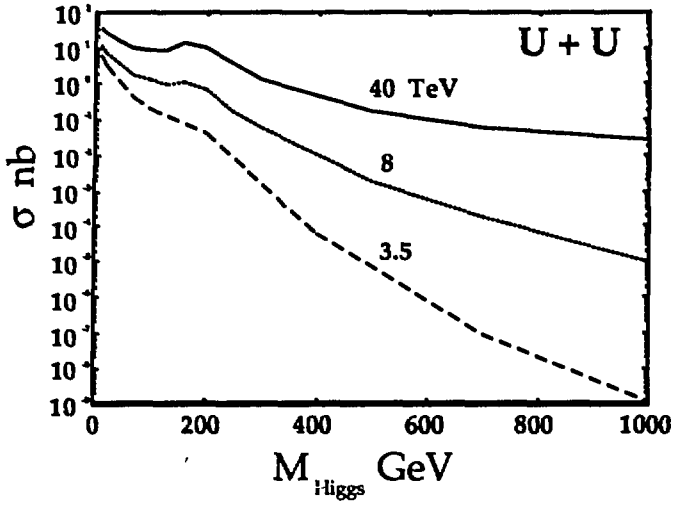

Fig. 11. Cross sections for production of the Higgs boson as a function of the Higgs mass.

the Higgs mass is unknown, the calculations must be performed for a range of possibilities. Figure 11 shows the cross section for uranium collisions as a function of mass at collider energies of 3, 8 and 20 TeV/nucleon. For an optimistic guess that the mass is 250 GeV/c^2, and the 8 TeV energy, corresponding to the Large Hadron Collider (LHC) at CERN (see Table 1), these calculations predict that 25 particles would be produced a year. This number is actually large enough to make the experiment worth thinking about further. In practice, numerous factors reduce the detection rate, but not drastically [13].

4. PORTABLE RANDOM NUMBER GENERATORS

In the course of performing the calculations described in Section 3.2, we encountered some difficulty in reproducing results from one machine to the other, due to

the lack of documented reliable random number generators (RNGs). The simple algorithms described in many textbooks were found to be inadequate for research purposes. We also felt the lack of methods suited to supercomputer architectures, which could generate statistically independent streams of random numbers by vector or parallel algorithms. To help others with similar problems, we shall outline the results of our investigations and experience. A more complete account will appear elsewhere [14]. We must also acknowledge a debt to the work of Percus and Kalos [15], who are among the very few people to have considered the problem of parallel RNGs.

All random numbers at the present day are produced by linear congruences, which paradoxically are completely predictable! These are usually written as a recurrence relation

$$x_{n+1} = ax_n + c \mod m \,, \tag{13}$$

where all quantities are integers, and m is as large as possible. It follows from elementary number theory that the maximum period of the congruence is m, and a large literature exists [16] on the conditions that this period is achieved if $m = p^q$ for p a prime, usually $p = 2$. Many books suggest "homemade" generators based on these conditions, such that a and c are obtained by truncating multiples of π or square roots. These generators have a distressing tendency to fail (by producing highly correlated numbers) for a simple reason. Unless a and c are examined closely, they may have a small factor in common with the result that all generated numbers have the same factor. This can be avoided by taking c from a large table

of prime numbers. We have also adopted the practice of taking the "seeds" x_0 from the same table. This prescription is sufficient to generate numerous independent parallel streams from given a and m [15]. A table of 10^4 or so primes is easily generated each time a large calculation is started.

The choice of m is dictated by the integer word length available. If complete portability of FORTRAN programs is required, $m \leq 2^{15}$. A longer period $\leq m^2$ is obtained by going to a two-term recurrence relation

$$x_{n+2} = a x_{n+1} + b x_n + c \mod m \,. \tag{14}$$

A good choice of a, b is best arrived at by an empirical search, in which standard tests are applied to a series of generators until a satisfactory one is identified. We shall now describe some tests, and the resulting generators, which we have found to be reliable in extensive applications.

The "chi-squared" test is one of the simplest and quite instructive [17]. A rectangular domain in one or more dimensions is divided into N boxes of equal size, as illustrated in Fig. 12 for 9 boxes in 2D. If the fraction in each box is f_j, the departure from a uniform distribution is measured by

$$\chi^2 = N \sum_{j=1}^{N} \left(f_j - \frac{1}{N} \right)^2 \,, \quad \sum_{j=1}^{N} f_j = 1 \,, \tag{15}$$

which is translated into a percentile on the standard distribution using the function $P(N|\chi^2)$ described in statistics textbooks. Some results are shown in Table 2 for three examples:

Table 2

Results of the chi-squared test for some random number generators.

RNG (defined in text)	N	Percentile
I	10^3	19 ± 6
II	10^3	44 ± 4
III	10^3	49 ± 3
I	10^4	13 ± 3
II	10^4	35 ± 9
III	10^4	49 ± 5

I A primitive homemade generator, with $a = 106, c = 1283, m = 6075$ in the notation of (13).

II The Vax intrinsic function **RAN**.

III One of our recommended portable generators, with $a = 25819, b = 22263, c = 991, m = 32749$ in the notation of (14).

In all cases we used 5^3 boxes in 3D and made six trial runs. A good generator lies in the range 40–60%. Notice that this is *not* a perfectly uniform distribution but a *random* deviation from one. The range 10–30% is adequate and $< 10\%$ should be shunned. It is instructive that the quality of I and II declines as the number of points increases. This is a matter of concern when we require 10^9 points in 8D, as in Section 3.2.

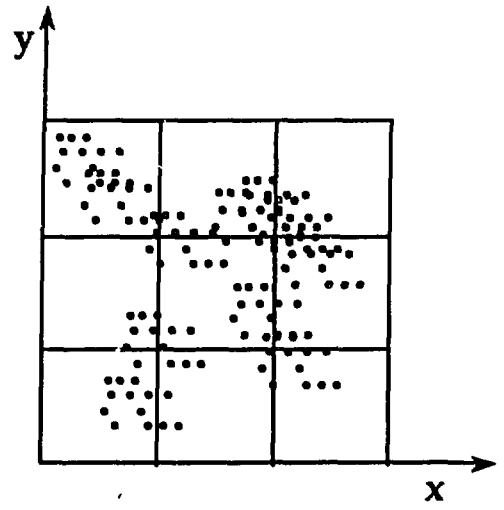

Fig. 12. Distribution of random points over bins for the chi-squared test.

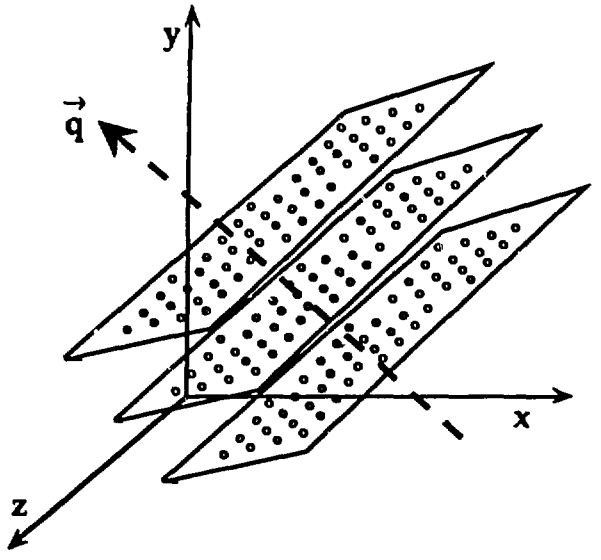

Fig. 13. Random points forming planes in 3D oriented according to $\vec{q}$.

The spectral test is regarded at the time of writing as the final word on the analysis of congruential random-number generators [17]. However, it is more difficult to implement and understand than the chi-squared test. The underlying principle is the observation that points in several dimensions generated by successive

terms of a congruence such as (13) must lie in hyperplanes defined by diophantine equations of the form,

$$\sum_{s=1}^{t} q_s a^{s-1} = 0 \mod m \,, \tag{16}$$

where t is the dimensionality. Equation (16) is appropriate for the form (13); the generalization to (14) requires some more writing, but involves no conceptual extensions [17]. Figure 13 illustrates schematically how such planes appear in 3D, and the geometric interpretation of the vector $\vec{q}$. The amount of space between the planes is measured by the inverse of the frequency

$$\nu_t = \min_{q} \left[\sum_{s=1}^{t} q_s^2 \right]^{1/2} \quad \forall\, q \text{ satisfying (16)} \,, \tag{17}$$

Such a minimum may be found with a modest amount of computation using theorems on quadratic forms due to Hermite. The larger ν_t, the better the generator, in the sense that large gaps in the filling of space are absent. It is customary to run the test for several dimensionalities, converting the results into figures of merit μ_t which scale out purely geometrical effects,

$$\mu_t = \frac{\pi^{t/2} \nu_t^t}{(t/2)!\, m^T} \,. \tag{18}$$

The number of terms in the congruence is denoted by T. Our portable generators have $T = 2$, corresponding to (14).

Results for three portable generators are shown in Table 3. The fourth entry supplies, for contrast, the analysis of the notorious URAND generator, widely used in the 1960's. It is generally considered that a generator is: excellent, satisfactory or inadequate according to whether $\mu_t > 1$, $\mu_t > 0.1$ or $\mu_t < 0.1$ for a series of

Table 3

Results of the spectral test for some random number generators. The constants a, b, m are as defined in (14) and $N = 2^{15}$ (N-19 is prime).

Parameters of RNG			Dimensionality				
a	b	m	2	3	4	5	6
25755	22263	N	3.14	2.07	4.40	4.36	4.30
25739	22263	$N-1$	3.14	2.40	1.07	0.47	0.81
25819	22263	$N-19$	3.14	1.80	1.50	1.27	1.25
$2N+3$	0	$N^2/2$	3.14	0.00	0.00	0.00	0.02

tests in dimensions $2 \leq t \leq 6$. Clearly the first and third generators in Table 3 win excellent ratings.

Finally, we have investigated the possibility of vectorized algorithms. Suppose we wish to generate a series of streams by vector instructions,

$$x_{n+1}(\alpha) = ax_n(\alpha) + c \bmod m \qquad \alpha = 1, \ldots, A\,. \tag{19}$$

Obviously the theorems on recursively generated streams do not apply to the sequence $\{x_n(\alpha)\}$, for n fixed. The best we can do is to take the seeds $x_0(\alpha)$ at random from a table initially generated sequentially, referred to as a "scramble table". It is usually stated that this procedure has no theoretical warranty, although it is observed to work very well. We have attempted to develop a theory of ensembles of RNGs, such as (19). This requires that we perform a series of spectral tests, with (16) replaced by

$$\sum_{s=1}^{t} q_s a^{\rho_s(\alpha)} = 0 \mod m \,, \tag{20}$$

where $\{\rho_s(\alpha)\}$ is a set of locations in the scramble table, each defining one stream α. We thereby obtain histograms, such as that in Fig. 14, showing the distribution

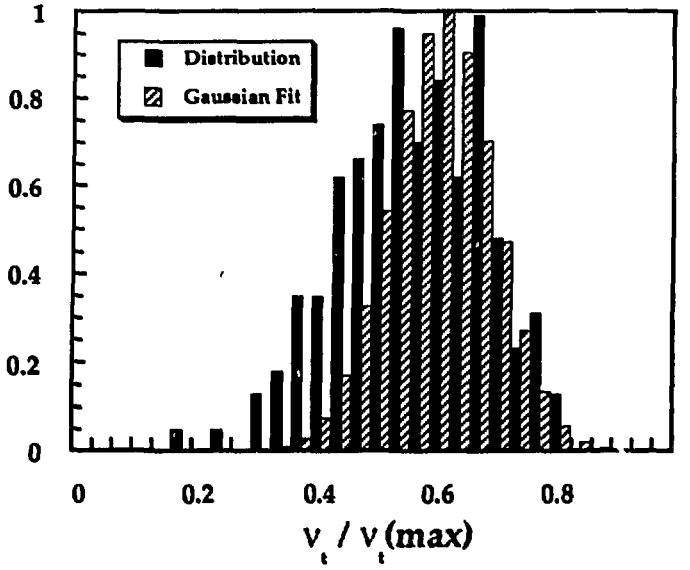

Fig. 14. Distribution of ν_t for an ensemble of RNGs, with a Gaussian fit for comparison. The abscissa is the ratio of ν_t to its theoretical maximum value $\nu_t(\max)$.

of ν_t values. These results were calculated from an ensemble of 5000 points in 5D, with the first generator of Table 3. The mean value of ν_t is close to that for the sequential generator $\rho_s = s - 1$, while the Gaussian distribution appears to be universal for a given dimension, with a width scaling as $t^{-1/2}$. We do not have a rigorous theory of these results, but they appear to justify the use of scramble tables, by showing that large gaps do not appear among the hyperplanes with a significant probability. The position is strengthened by a further result of our calculations that the vectors $\vec{q}_{\min}$ defining the closest planes are randomly oriented, so that no spaces are unfilled when all streams are superimposed.

5. ACKNOWLEDGEMENTS

This research was sponsored by the Division of Nuclear Physics, U.S. Department of Energy under contract No. DE-AC05-84OR21400 with Martin Marietta Energy Systems, Inc., and by the Division of Chemical Sciences, Office of Basic Energy Sciences.

REFERENCES

1. Frank Close, *The Cosmic Onion*, (American Institute of Physics, New York, 1985).

2. "Proceedings of the 4th RHIC Workshop", Brookhaven National Laboratory, July 2–7,1990, edited by M. Fatyga and B. Moskowitz, BNL 52262.

3. "Proceedings of the ICFA Seminar on Future Perspectives in High-Energy Particle Physics", edited by P.F. Dahl, (American Institute of Physics, Brookhaven, NY, 1987).

4. C. Bottcher and M.R. Strayer, in "Physics of Strong Fields", ed. W. Greiner, (Plenum, New York, 1987), Vol. **153**, p. 629; "Proceedings of the Second Workshop on Experiments and Detectors for the RHIC", Berkeley, CA, May 25-29, 1987, p. 279, (LBL-24604).

5. J. D. Bjorken and S. D. Drell, *Relativistic Quantum Mechanics*, (McGraw-Hill, New York, 1964); C. Itzykson and J.-B. Zuber, *Quantum Field Theory*, (McGraw-Hill, New York, 1980); Vernon Barger and Roger Phillips, *Collider*

Physics, (Addison-Wesley, New York, 1987).

6. C. Bottcher and M.R. Strayer, Phys. Rev. **D39**, 1330 (1989); Nucl. Inst. and Meth. **B31**, 122 (1988); Nucl. Inst. and Meth. **B40**, 354 (1989); J.S. Wu, C. Bottcher and M.R. Strayer, Phys. Rev. **C43**, 2422 (1991); C. Bottcher and M.R. Strayer, in "Proc. of the Summer School of Computational Atomic and Nuclear Physics", p 118, (World Scientific, Teaneck, NJ, 1990).

7. G. Baur and C.A. Bertulani, Phys. Rep. **161**, 299 (1988); J. Rau, B. Müller, W. Greiner and G. Soff, J. Phys. **G15**, L25 (1989); G. Racah, Nuovo Cimento, **14**, 70 (1937).

8. C. Bottcher, M. J. Rhoades-Brown and M. R. Strayer, in "Proceedings of Workshop on Highly Charged Ions: New Physics and Advanced Techniques", Berkeley, CA, March 13-15, Nucl. Instrum. & Meth. in Phys. Res. **B43**, 301-5 (1989); C. Bottcher and M. R. Strayer, in "Proceedings of Workshop: Can RHIC be used to test QED?", Brookhaven National Laboratory, April 20–21, 1990, edited by M. Fatyga, M.J. Rhoades-Brown and M.J. Tannenbaum, BNL 52247.

9. C. Bottcher, M.J. Rhoades-Brown and M. R. Strayer, Phys. Rev. **A40**, 2831-34 (1989)

10. M.J. Rhoades-Brown, T. Ludlam, J.S. Wu, C. Bottcher and M. R. Strayer, in "Proceedings of the 4^{th} RHIC Workshop", Brookhaven National Laboratory, July 2–7,1990, edited by M. Fatyga and B. Moskowitz, BNL 52262.

11. Elena Papageorgiu, Phys. Rev. **D40**, 92 (1989); Nucl. Phys. **A498**, 593c (1989); M. Drees, J. Ellis and D. Zeppenfeld, Phys. Lett. **B223**, 454 (1989); M. Grabiak, B. Müller, W. Greiner, G. Soff, and P. Koch, J. Phys. **G15**, L25 (1989).

12. J.S. Wu, C. Bottcher, M. R. Strayer and A.K. Kerman, Particle World, **1**, 174 (1990).

13. R.N. Cahn and J.D. Jackson, Phys. Rev. **D40**, 3690, (1990); B. Müller and A.J. Schramm, Phys. Rev. **D40**, 3696, (1990); M.S. Chanowitz, *Electroweak symmetry breaking studies at the pp colliders of the 1990's and beyond*, Lawrence Berkeley Laboratory preprint LBL-28592 (1990); J.S. Wu, C. Bottcher, M. R. Strayer, A.K. Kerman, to appear in Ann. Phys. (N.Y.), 1991.

14. G. Arbanas, C. Bottcher and M. R. Strayer, in preparation.

15. O.E. Percus and M.H. Kalos, J. Parallel Dist. Comp. **6**, 477 (1989).

16. Birger Jannson, *Random Number Generators*, (Almqvist Wiksell, Stockholm, 1966)

17. D.E. Knuth, *The Art of Computer Programming*, volume 2 — *Seminumerical Algorithms*, (Addison-Wesley, Reading MA, 2nd edition, 1981). Note: the first edition (1969) gave a different treatment of the spectral test which is still worth consulting.